IMPACT OF TERRAIN AWARE INTERFERENCE MODELING ON THE THROUGHPUT OF COGNITIVE Ka-BAND SATELLITE SYSTEMS

Eva Lagunas, Shree Krishna Sharma, Sina Maleki, Symeon Chatzinotas and Björn Ottersten

Interdisciplinary Center for Security, Reliability and Trust (SnT), University of Luxembourg
4, rue Alphonse Weicker L-2721 Luxembourg
{eva.lagunas,shree.sharma,sina.maleki,symeon.chatzinotas,bjorn.ottersten}@uni.lu

Abstract

The impact of including the diffraction loss in the interference modeling on the system throughput is assessed in the context of cognitive Ka-band satellite systems. In particular, we focus on the cognitive satellite downlink, where Geostationary (GEO) Fixed Satellite Service (FSS) terminals receive interference from the incumbent Fixed-Service (FS) microwave links. We present numerical results where we analyze the Signal-to-Interference plus Noise Ratio (SINR) and the throughput of the satellite terminals considering free-space propagation only and the free-space propagation plus the diffraction caused by the terrain data according to ITU-R P.526-13. We also compare the results achieved with and without smart resource allocation. The inclusion of the diffraction loss is shown to attenuate the interference caused by the terrestrial system and thus, to improve the SINR of the satellite terminals. However, its effect on the final throughput has little relevance due to the significant number of available and unaffected carriers.

1. Introduction

Cognitive satellite communications has been recognized as a promising way to improve spectrum efficiency of broadband Ka-band satellite systems by exploiting under-utilized spectrum licensed to terrestrial systems [1-3]. The coexistance between satellite and terrestial systems has recently attracted significant research interest [4-7]. Accurate interference modelling is fundamental when evaluating the potential of spectrum coexistence between satellite and terrestrial systems.

In this paper, we evaluate the impact of terrain and diffraction loss when modelling the interference caused by the incumbent Fixed-Service (FS) microwave links to the cognitive downlink access by Geostationary (GEO) Fixed Satellite Service (FSS) terminals in the band 17.7-19.7 GHz. More precisely, we consider the effect of accurate interference modelling into the achievable satellite throughput. The present paper is a continuation of the our previous work [8], where we modelled the propagation loss as a simple line-of-sight path through free space path-loss model, with no obstacles nearby to cause diffraction. The consequences of considering terrain data into the interference modelling has been studied in [9-11] for the 17.7-19.7 GHz band but without providing information on the Signal-to-Interference and Noise Ratio (SINR), and on the achievable throughput. In this context, we provide detailed numerical results to compare both SINR and achievable throughput in the following cases: (i) considering the diffraction loss, which takes into account terrain data, (ii) the free space loss model, which only includes line of sight propagation loss. We will also evaluate the effect of diffraction with and without considering the smart resource allocation algorithm proposed by the authors in [8].

Numerical results show that, although the carriers affected by interfering FS links are limited due to terrain diffraction, there are still many free-of-interference carriers which can be allocated to the cognitive FSS terminal users.

This paper is part of the activities carried out in the frame of FP7 CoRaSat project [3], where cognitive radio enablers for the identified scenario will be developed and demonstrated for specific use cases through analysis, simulation, and testbed implementation.

The remainder of this paper is organized as follows. In Section II, the scenario and the interference modeling approach are introduced. In Section III, we briefly review the carrier allocation strategy proposed by the authors in [8]. In Section IV, numerical results are shown to analyze the performance of the cognitive satellite system in terms of SINR and throughput. Finally, Section V concludes the paper.
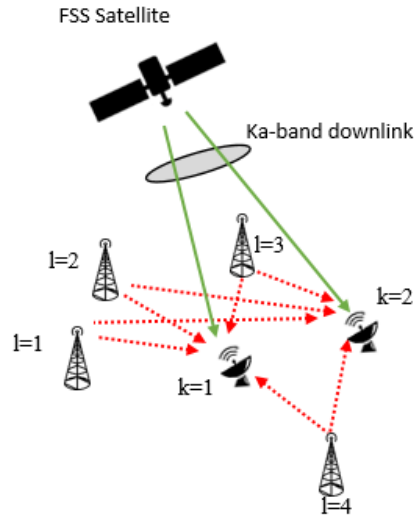
Fig. 1 Spectral coexistence of FSS donwlink with the FS microwave links in the Ka-band (17.7-19.7 GHz)

2. Scenario Description and Cognitive Exploitation Framework

2.1 Scenario Description

Fig. 1 depicts the considered scenario, where the cognitive satellite downlink operates in the band 17.7-19.7 GHz, which is assigned to the incumbent FS microwave links. The interference is from the FS links to the FSS receive terminals. The deployment of FS microwave links in the 17.7-19.7 GHz band is large (e.g. 13,000 in the UK) so there will be many interference paths. However, not all of them will cause interference at a particular site due to the very narrow beam and extremely directional transmissions of FS microwave links, which are generally deployed for backhauling point-to-point application [11]. Note that the downlink interference from the cognitive satellite to the terrestrial FS receivers is negligible due to the limitation in the maximum Effective Isotropic Radiated Power (EIRP) density of the current Ka band satellite system [12].

2.2 Exploitation Framework

The block diagram of the proposed exploitation framework is sketched in Fig. 2
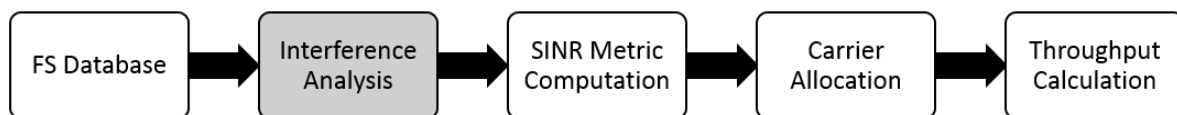

Fig. 2 Block diagram of the cognitive exploitation framework

We assume the availability of a complete and reliable FS database, with information on the location of the FS antennas, transmission powers, antenna pointing, frequency and bandwidth. This information is used in to determine the interference level at each of the FSS terminal receivers. In this paper, we compare two ways of modeling the propagation loss: (i) the conventional free space path loss based on the simple line-of-sight model, and (ii) a more complete model which takes into account the terrain data of the area under evaluation by means of the diffraction loss component. Once the interference levels are obtained, and using the link budget information of the satellite downlink, the SINR is computed for each FSS terminal considering all carrier frequencies. According to the values of SINR, an optimal carrier allocation algorithm can be implemented in order to maximize the cognitive satellite downlink throughput [8]. The last block computes the througput according to the received carrier allocation.

3. Signal Model

3.1 Interference Characterization

We consider a scenario with K FSS terminal users and L FS microwave transmitters. The received interference from the L FS microwaves transmitters at the k-th FSS terminal for a particular carrier frequency f_m, $m = 1, \ldots, M$, is given by,

$$I(m,k) = \sum_{l=1}^{L} I(m,k,n),\qquad(1)$$

where $I(m,k,n)$ denotes the interference level caused by a single l-th FS terminal at the m-th carrier frequency under consideration. The latter can be written as,

$$I(m,k,n) = P_{FS}^{TX}(l) \cdot G_{FS}^{TX}(\theta_{l,k}) \cdot G_{FSS}^{RX}(\theta_{k,l}) \cdot L,\qquad(2)$$

where,

- $P_{FS}^{TX}(l)$ denotes the transmit power of the l-th FS transmitter.
- $G_{FS}^{TX}(\theta_{l,k})$ denotes the gain of the l-th FS transmitting antenna at an offset angle θ. Its radiation pattern can be obtained from ITU-R F.1245-2.
- $G_{FSS}^{RX}(\theta_{k,l})$ denotes the gain of the k-th FSS terminal antenna at an offset angle θ. Its radiation pattern can be obtained from ITU-R S.465-6.
- $\theta_{i,j}$ denotes the offset angle (from the boresight direction) of the i-th station in the direction of the j-th station.
- L denotes the propagation loss, which here will be modeled in two ways:

  i. $L = L_{FSPL} = \left(\dfrac{c}{4\pi d f}\right)^2$ which corresponds to the free space path loss model with d beign the transmitter-receiver distance, f being the carrier frequency and c being the speed of the light.

  ii. $L = L_{FSPL} + L_{dif}$, where L_{dif} denotes the diffraction loss, which is modeled following the recommendation ITU-R P.526-13 "Propagation by diffraction". More precisely, we use the Bullington model for a general terrestrial path [13, Section 4.5.1].

Note that (2) assumes perfect matching between the interfering signal bandwidth and the victim bandwidth. In practice, however, this is not the case. In this paper, a compensation factor of $\dfrac{B_{overlap}}{B_{FSS}}$ is applied, where $B_{overlap}$ stands for the portion of the interfering signal spectrum within the received filter bandwidth given by B_{FSS}.

3.2 SINR Calculation

The SINR corresponding to the k-th FSS terminal operating at the m-th carrier frequency is given by,

$$SINR(m,k) = \frac{P_{FSS}^{RX}(k)}{I(m,k) + I_{co} + N_0},\qquad(4)$$

where I_{co} is the interference caused by signals transmitted in cochannel beams of a multi-beam satellite, N_0 is the noise thermal power calculated over B_{FSS} and $P_{FSS}^{RX}(k)$ denotes the received signal power at the k-th FSS terminal, which can be obtained as follows,

$$P_{FSS}^{RX}(k) = P_{SAT}^{TX}(k) \cdot G_{SAT}^{TX}(k) \cdot G_{FSS}^{RX}(0) \cdot L_{FSPL}.\qquad(5)$$

In (5), $P_{SAT}^{TX}(k)$ denotes the transmit power of the FSS satellite, $G_{SAT}^{TX}(k)$ is the beam gain for the k-th FSS terminal user and $G_{FSS}^{RX}(0)$ denotes the FSS terminal antenna gain at the boresight direction.

4. Carrier Allocation

In this paper, we also evaluate the effect of diffraction with and without considering the smart resource allocation algorithm proposed by the authors in [8]. This section reviews the carrier allocation algorithm presented in [8]. The technique presented in [8] assumes the availability of the SINR values per user and per carrier at the Network Control (NC) of the satellite system. These SINR values can be stacked in matrix form as follows,

$$\mathbf{SINR} = \begin{bmatrix} SINR(1,1) & \cdots & SINR(1,K) \\ \vdots & \ddots & \vdots \\ SINR(M,1) & \cdots & SINR(M,K) \end{bmatrix}, \tag{6}$$

where the rows indicate carrier frequencies and the columns indicate the FSS terminal users. The goal of [8] is to maximize the sum-rate of the satellite system. The user-rates per carrier frequency, namely $\mathbf{R}(\mathbf{SINR})$, can be obtained from the SINR values with the table provided in DVB-S2X standard [14]. The dimensions of $\mathbf{R}(\mathbf{SINR})$ are $M \times K$.

Let $a(m,k) = \{0,1\}$ be the (m,k)-th element of an $M \times K$ carrier allocation matrix $\mathbf{A}$, the technique presented in [8] determines the value of $\mathbf{A}$ that solves the following optimization problem,

$$\max_{\mathbf{A}} \quad \|\mathrm{vec}(\mathbf{A} \bullet \mathbf{R}(\mathbf{SINR}))\|_1$$
$$\text{subject to} \quad \sum_{m=1}^{M} a(m,k) = 1 \tag{7}$$

where $\bullet$ denotes the Hadamard product, $\mathrm{vec}(\cdot)$ denotes the vectorization operator and $\|\cdot\|_1$ denotes the l_1-norm. We solve the optimization problem in (10) using the Hungarian algorithm [15], which provides an efficient and low complexity method to solve the one-to-one assignment problem in polynomial time.

5. Numerical Results

5.1 Simulation Results considering real FS deployment

The parameters related to the FS microwave links are obtained from ITU-R BR International Information Circular (BRIFIC) database [16]. The database includes information on the geographical location of each antenna, its transmit power, its maximum antenna gain and the corresponding channel bandwidth.

We focus on the database of France, with more than 12,000 entries. A real FSS satellite beam pattern providing coverage over France is obtained from Thales Alenia Space. Both $G_{SAT}^{TX}(k)$ and I_{co} can be extracted from the provided beam pattern. In this paper, we focus on the beam providing coverage over the region of Marseille, which corresponds to a highly populated area. Fig. 2 illustrates the beam pattern and the FS distribution over the region of Marseille.

The results obtained in this section were obtained after 50 Monte Carlo runs, in which the locations of the FSS terminals were randomly selected for each realization according to the French population density database. The simulation parameters are summarized in Table 1.

Table 1. Simulation parameters

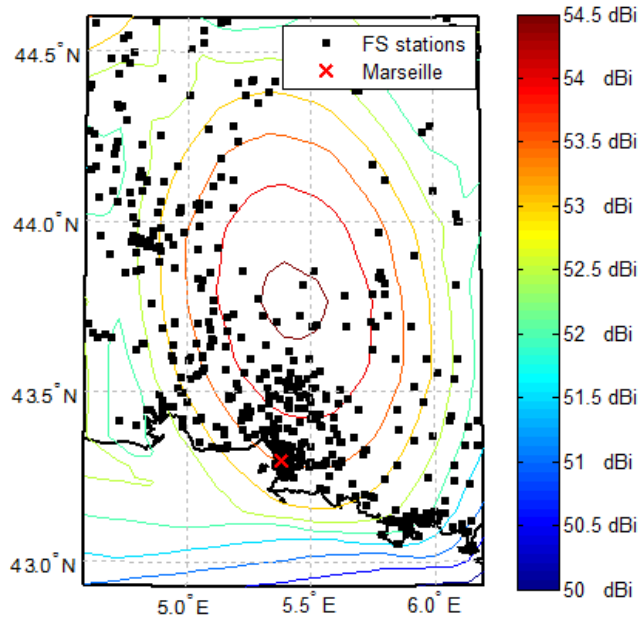| Parameter	Value
B_{FSS}	62.4 MHz
Shared band	17.7-19.7 GHz (32 carriers)
Exclusive band	19.7-20.2 GHz (8 carriers)
Satellite	13˚E
EIRP satellite	65 dBW
Reuse satellite pattern	4 color (freq./pol.)
$G_{FSS}^{RX}(0)$	42.1 dBi
N_0	-126.46 dBW
Terminal height	15 m

Fig. 2 Beam pattern and FS distribution over Marseille region.

The effect of FS interference on the SINR of the FSS terminals is depicted in Fig. 3 in terms of Cumulative Distribution Function (CDF). In Fig. 3, we depict three different cases: (i) when the FS microwave stations are not present (black line); (ii) when the interference between FS transmitters and FSS terminals is modeled with a simple free space path loss (black line); and (iii) when the interference between FS transmitters and FSS terminals considers diffraction on top of the free space path loss. It can be observed that the SINR degrades in the presence of FS transmitters. In particular, 28% of users experience values of SINR below 10 dB when the FS transmitters are not present, which increases up to 36,4% when interference is modeled with free space path loss plus diffraction loss, and up to 40,6% when diffraction is neglected. Although the carriers affected by interfering FS links are limited due to terrain diffraction, there are still many free-of-interference carriers which can be allocated to the FSS terminal users. This is evident by a glance of Fig. 4, where the SINR per carrier frequency for different realizations is shown. Clearly, only a few carriers experience low levels of SINR when no FS stations are considered.
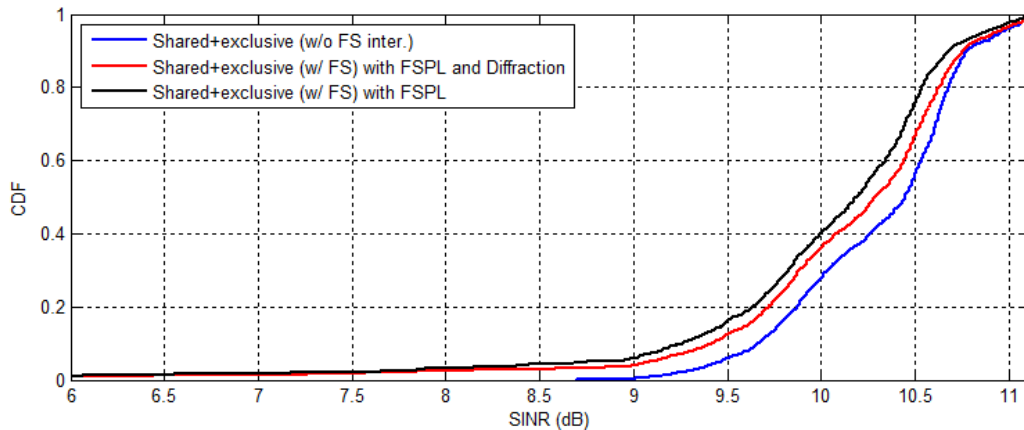

Fig. 3 CDF of SINR distribution.

Finally, Table 2 presents the throughput per beam comparison. We compare four different cases; the same three as in Fig. 3 plus a case where only the exclusive 500 MHz of bandwidth is assumed available for the satellite downlink. As expected, the throughput significantly increses when considering the 2 GHz of extra bandwidth. However, the diffraction effect based on the terrain data is not significant on the final throughput of the system, which increases less than 1% in comparison to the case when diffraction is neglected. Moreover, Table 2 compares the optimal CA introduced in [8] with a random CA and the worst possible CA, i.e., assigning the users to the carriers with lowest SINR. It can be seen that the optimal CA introduced in [8] can efficiently allocate most of the users to

interference-free carriers and, thus, achieving a beam throughput close to the ideal case in which FS transmitters are not present. Even considering the worst CA, the throughput difference is less than 1%.

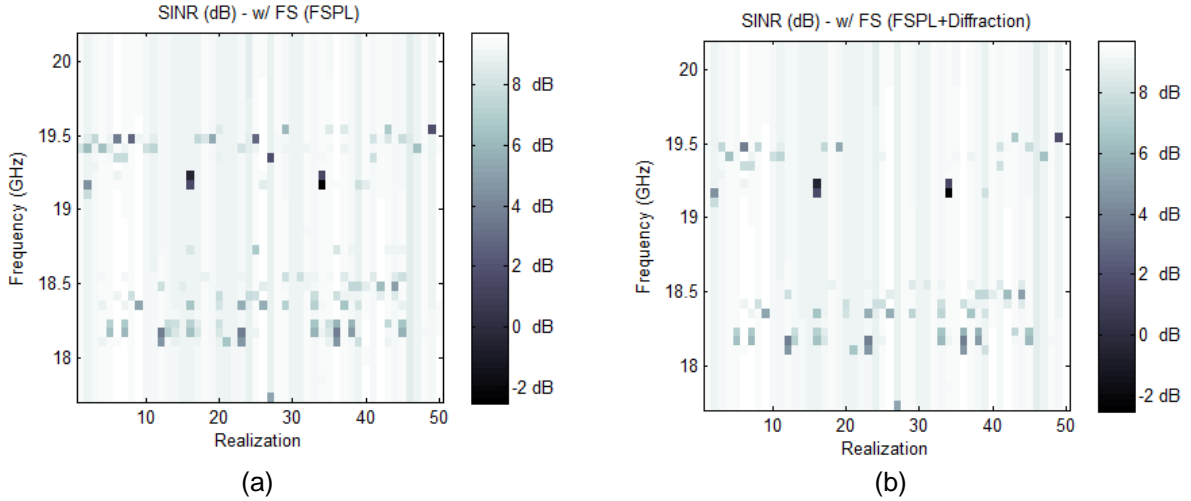(a)   (b)

Fig. 4 SINR per carrier frequency for different realizations: (a) with free space path loss, and (b) with free space path loss and diffraction loss.

Table 2. Throughput per beam results (Mbps)

	Case CA	Worst CA	Random CA	Optimal CA
	Exclusive only	725.79	726.13	726.68
Propagation model	Shared+Exc. w/o FS	3612.16	3630.85	3650.57
FSPL	Shared+Exc. w/ FS	3530.09	3626.13	3650.29
FSPL + Diffraction		3557.48	3627.67	3650.43
Gain when considering diffraction over FSPL only	Shared+Exc. w/ FS	0.770%	0.057%	0.004%

5.2 Simulation Results considering future FS deployment

To simulate a future FS deployment, we artificially increase the number of entries of the ITU BRIFIC database used in Section 5.1. To do so, we apply a mirroring effect to each of the originally listed links as Fig. 5 indicates. Basically, only the azimuth is change while keeping all other parameters equal to the original link.

The CDF of the SINR of the FSS terminals is depicted in Fig. 6. In this case, 51,2% of users experience values of SINR below 10dB when interference is modeled with free space path loss plus diffraction loss, which increases up to 60,95% when diffraction is neglected.

Table 3 presents the throughput per beam achieve for the future FS deployment. Increasing the number of interfering FS links increase the number of affected carriers but yet its effect in the final throughput is still rather insignificant. The effect of the diffraction loss translates into a 1.5% increase in final throughput in comparison with the free space path loss only case. Again, the smart carrier allocation [8] is still able to assign most of the users to interference-free carriers, thus, making the diffraction effects almost invisible to the end users.
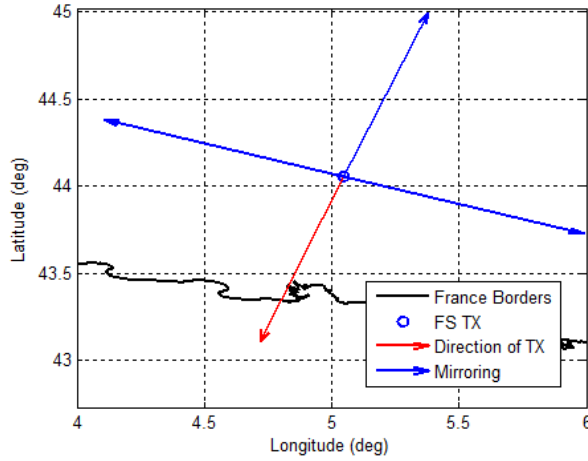
Fig. 5 Mirroring technique used to artificially simulate a future FS deployment.
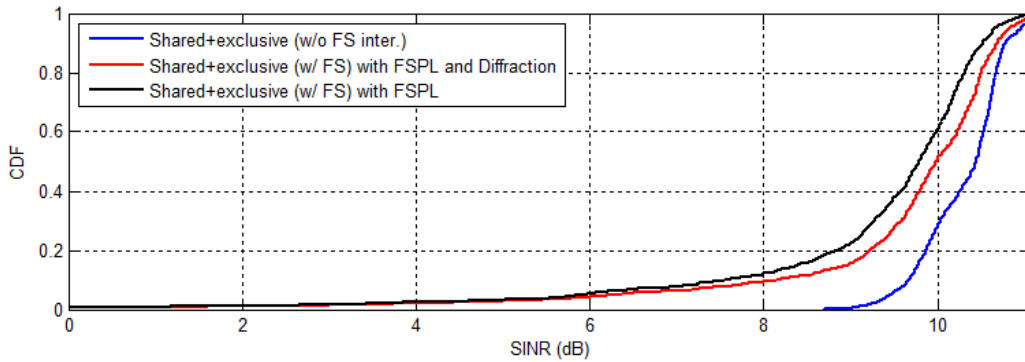

Fig. 6 CDF of SINR distribution for the future FS deployment case.

Table 3. Throughput per beam results for future FS deployment (Mbps)

	Case＼CA	Worst CA	Random CA	Optimal CA
	Exclusive only	725.8	726.1	726.7
Propagation model	Shared+Exc. w/o FS	3612.2	3630.9	3650.6
FSPL	Shared+Exc. w/ FS	3388.9	3614	3649.3
FSPL + Diffraction		3439	3621.4	3650.2
Gain when considering diffraction over FSPL only	Shared+Exc. w/ FS	1.478 %	0.205 %	0.025 %

5. Conclusions

In this paper, we analysed the impact of including the radio propagation effect of diffraction in the performance of the cognitive satellite downlink in the 17.7-19.7 GHz band where FS microwave links have priority of protection. We show through numerical simulations that the diffraction loss attenuates the interference caused by FS microwave links and, thus, higher SINR and higher throughput gains can be achieved, which is in line with the conclusions in [9-11]. However, although the carriers affected by interfering FS links are limited due to terrain diffraction, there are still many free-of-interference carriers which can be allocated to the FSS terminal users. Therefore, carrier allocation techniques are still able to assign most of the users to interference-free carriers, thus, making the diffraction effects almost invisible to the end users.

ACKNOWLEDGMENT

References

[1] Maleki, S.; Chatzinotas, S.; Evans, B.; Liolis, K.; Grotz, J.; Vanelli-Coralli, A.; Chuberre, N., "Cognitive spectrum utilization in Ka band multibeam satellite communications," Communications Magazine, IEEE , vol.53, no.3, pp.24,29, March 2015.

[2] Biglieri, E., "An overview of Cognitive Radio for satellite communications," IEEE AESS European Conf. Satellite Telecommunications (ESTEL), Rome, Italy, Oct. 2012

[3] A. Vanelli-Coralli, A. Guidotti, D. Tarchi, S. Chatzinotas, S. Maleki, S. Sharma, N. Chuberre, B. Evans, M. Lopez-Benitez, W. Tang, J. Grotz, and K. Liolis, *Cooperative and Cognitive Satellite Systems*. Oxford, UK: Academic Press, 2015, chapter *Cognitive Radio Scenarios for Satellite Communications: The CoRaSat Project*.

[4] M. Hoyhtya, J. Kyrolainen, A. Hulkkonen, J. Ylitalo, and A. Roivainen, "Application of Cognitive Radio Techniques to Satellite Communication," IEEE Symp. on Dynamic Spectrum Access Networks (DySPAN), Bellevue, WA, USA, Oct, 2012.

[5] S. Vassaki, M.I. Poulakis, A.D. Panagopoulos, "Optimal iSINR-based power control for cognitive satellite terrestrial networks", Trans. on Emerging Telecommunications Technologies, Mar 2015.

[6] S. Sharma, S. Maleki, S. Chatzinotas, J. Grotz, J. Krause, and B. Ottersten, "Joint Carrier Allocation and Beamforming for Cognitive Satellite Communications in Ka-band (17.3-18.1 GHz)," IEEE Int. Conf. on Communications (ICC), London, UK, Jun, 2015.

[7] E. Lagunas, S. Sharma, S. Maleki, S. Chatzinotas, J. Grotz, J. Krause, and B. Ottersten, "Resource Allocation for Cognitive Satellite Uplink and Fixed-Service Terrestrial Coexistence in Ka-band," Int. Conf. on Cognitive Radio Oriented Wireless Networks (CROWNCOM), Doha, Qatar, Apr, 2015.

[8] S.K. Sharma, E. Lagunas, S. Maleki, S. Chatzinotas, J. Grotz, J. Krause, B. Ottersten, "Resource Allocation for Cognitive Satellite Communications in Ka-band (17.7-19.7 GHz)", Workshop on Cognitive Radios and Networks for Spectrum Coexistence of Satellite and Terrestrial Systems, IEEE Int. Conf. On Communications (ICC), London, UK, Jun 2015.

[9] W. Tang, P. Thompson, B. Evans, "Frequency Sharing between Satellite and Terrestrial Systems in the Ka Band: A Database Approach", IEEE Int. Conf. Comm. (ICC), London, UK, Jun 2015.

[10] P. Thompson, B. Evans, "Analysis of Interference between Terrestrial and Satellite Systems in the Band 17.7 to 19.7 GHz", Workshop on Cognitive Radios and Networks for Spectrum Coexistence of Satellite and Terrestrial Systems, IEEE Int. Conf. On Communications (ICC), London, UK, Jun 2015.

[11] W. Tang, P. Thompson, B. Evans, "A Database Approach to Extending the Usable Ka Band Spectrum for FSS Satellite Systems", Int. Conference on Advances in Satellite and Space Communications (SPACOMM), Barcelona, Spain, Apr 2015.

[12] S. Sharma, S. Maleki, S. Chatzinotas, J. Grotz, and B. Ottersten, "Implementation Issues of Cognitive Radio techniques for Ka-band (17.719.7 GHz) SatComs," Adv. Sat. Multimedia Systems (ASMS) Conf. and Signal Processing for Space Comm. (SPSC) Workshop, Livorno, Italy, Sep, 2014.

[13] ITU-R P.526-13 (11/2013) Propagation by Diffraction. Available online at: http://www.itu.int/rec/R-REC-P.526-13-201311-I

[14] DVB-S2X Standard, Available online at: https://www.dvb.org/standards/dvb-s2x

[15] H. Kuhn, "The Hungarian Method for the Assignment Problem", Naval Research Logistics Quarterly, vol. 2, pp. 83-97, 1955.

[16] ITU, BR IFIC for terrestrial services. Available at: http://www.itu.int/en/ITU-R/terrestrial/brific